



TIME-DEPENDENT THERMAL-MATERIAL TRANSFER OF MICROPOLAR BINARY MIXTURE FLUID: EFFECTS OF LORENTZ FORCE AND INCLINATION

Md. Mosharrof Hossain¹, Md. Hasanuzzaman² and R. Nasrin³

Department of Mathematics, Bangladesh University of Engineering & Technology,

Dhaka-1000,Bangladesh

¹E-mail: mosharrofs77@gmail.com

³E-mail: rehena@math.buet.ac.bd

²Department of Mathematics,

Khulna University of Engineering & Technology,

Khulna-9203, Bangladesh

E-mail: hasanuzzaman@math.kuet.ac.bd

ABSTRACT

The effects of Lorentz force and inclined angle on time-dependent free-convective thermal-material transport by micropolar binary mixture of fluid passing a continuous permeable surface have been analyzed in this article. Using the local similarity transformation, the governing partial differential equations have been converted into ordinary differential equations. The shooting technique was then employed to solve non-dimensional ordinary differential equations with boundary conditions using the "MATLAB ODE45" software. The effects of emerging Lorentz force (M) and inclined angle (γ) on the fluid velocity, concentration, temperature, and microrotation have been investigated within the boundary layer. Other non-dimensional parameters in this study, such as Schmidt number, suction parameter, and Prandtl number are kept fixed at Sc=0.22, c=0.5, and Pr=0.71, respectively. The numerically simulated result shows that the velocity falls for uplifting values of the inclined angle and Lorentz force. The skin friction coefficient decreases by 49%, and 20% due to increasing the values of inclined angle (0°-60°), and Lorentz force (1.0 - 4.0), respectively. The surface couple stress is found to be increased about 24%, and 44% with the upturning values of M (1.0 - 4.0), and γ (0°-60°), respectively. Through this research, the behavior of the fluid flow has been explored.

Keywords: Micropolar binary mixture fluid; Lorentz force; Inclination; Thermal-material transfer; Time-dependent analysis.

1. INTRODUCTION

A class of fluids that display specific microscopic effects resulting from the micromotions of the fluid components are covered by the theory of micropolar fluid. Such fluids can be used to study the behavior of liquid crystals, animal blood, unusual lubricants, colloidal suspensions, or polymeric fluids, for instance respectively. In the fields of chemical engineering, aeronautical engineering, as well as the investigation of heat and mass transfer in micropolar fluids, industrial manufacturing processes is significant. Cheng [1] has analyzed the problem of convective heat and mass transport in a vertical channel with asymmetric wall temperatures and concentrations. According to Haque et al. [2] the motion of micropolar fluid is more noticeable for lighter particles and air compared to heavier particles and water respectively. By using numerical analysis, Ali et al. [3] studied the boundary layer nanofluid flow over a stretching permeable wedge-shaped surface with magnetic effect. According to Tripathy et al. [4], a rise in magnetic parameter, porous matrix, and inertial influence causes an improvement in skin friction, but an increase in material parameter results in a decrease. The problem of unsteady convection with chemical reaction, thermophoresis, and radiative heat transfer in a micropolar fluid which flows through a vertical

permeable surface passing by a binary mixture was studied by Animasaun [5] while taking temperature dependent dynamic viscosity and constant vortex viscosity into consideration.

Magnetohydrodynamics (MHD) is the study of the electrically conducting behavior of fluids in the presence of a magnetic field. The Lorentz force is the result of electromagnetic fields' combined application of magnetic and electric forces on a point charge. Immaculate et al. [6] talked about the effect of thermophoretic particle deposition on mixed convective flow of heat and mass transport. It was considered in a vertical channel with radiative heat flux and diffusion-thermo and thermal-diffusion impacts due to magnetic field. Ahmed et al. [7] observed the influences of Soret unstable free convective flow of an electrically conducting fluid over an infinitely long, oscillating plate encased in a porous media with uniform transverse magnetic field. Vedavathi et al. [8] analyzed the combined effects of heat and mass transfer on two-dimensional unsteady free convection flow. They considered the presence of a magnetic field through a vertical porous plate in a porous material in the presence of thermal radiation. Prasad et al. [9] has looked into the impact of Soret on the flow of an unsteady magnetohydrodynamic mixed convective heat and mass transfer in a permeable surface surrounding an accelerated vertical wavy plate while

taking into account the angle of inclination, Casson fluid, chemical reaction, and thermal radiation. The Falkner-Skan boundary-layer problem for a moving wedge submerged in a nanofluid with magnetic field was studied by Ali et al. [10].

passing nanofluid flow The of electromagnetic plate was described by Rasool and Wakif [11]. Investigations have been conducted by Asogwa et al. [12] on the incompressible, transient free convective, electromagnetohydrodynamic flow of the Casson fluid across a porous medium with constant concentration and temperature in the presence of a heat sink, diffusion thermo, and thermal diffusion. Ali et al. [13] investigated the impacts of dimensionless parameters on the temperature field, nanoparticle concentration field, and velocity field. The capacity of a material to conduct heat is measured by its thermal conductivity. High thermal conductivity materials may easily absorb heat from their surroundings and effectively transport heat between them. Poor thermal conductors delay heat transfer and absorb heat slowly from their environment. In a generalized thermoelasticity environment without energy dissipation. Li et al. [14] investigated the transient thermoelastic responses of bi-layered skin tissue with temperaturedependent thermal material characteristics. Kowsalya and Begam [15] investigated the MHD mass transfer flow across a vertical permeable surface contained in a porous medium under the impact of heat diffusion and the hall current in a slip flow regime. The novelty of this research work is increased further by considering the continuous permeable surface with the effects of Lorentz force and inclined angle which has not been discussed yet.

2. MATHEMATICAL ANALYSIS

We study an unstable magneto-convective heat-mass transfer of a micropolar binary fluid mixture over a continuous permeable surface. Across the x-axis, the flow is taken into account. This is also assumed along the semi-infinite surface, and the y-axis is perpendicular to it. When the absorption coefficient (α) meets the requirement α << 1, an optically thin fluid is taken into consideration. According to Cheng [16], the fourth power of temperature in the energy balance equation roughly describes the radiative heat flux $\frac{\partial q_r}{\partial y}$. According to boundary layer theory, the temperature gradient normal to the surface is substantially greater than the temperature gradient along the surface.

i.e.,
$$\frac{\partial T}{\partial y} \gg \frac{\partial T}{\partial x}$$

For this reason, the thermophoretic velocity component along the surface is ignorable with comparison to velocity component normal to the surface. It is expected that the free stream temperature T_{∞} is higher than the wall temperature (T_w) $(T_{\infty} > T_w)$. With the help of all presumptions expressed above and Boussinesq's approximation; the governing equations can be written as:

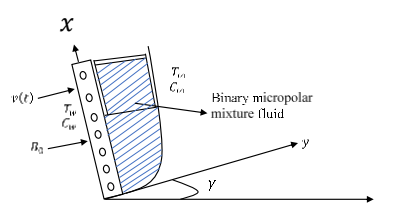


Figure 1: Physical Model and coordinate system

$$\frac{\partial v}{\partial y} = 0$$

$$\frac{\partial u}{\partial t} + v \frac{\partial u}{\partial y} = \left(\frac{\mu + \tau}{\rho}\right) \frac{\partial^2 u}{\partial y^2} + \frac{\tau}{\rho} \frac{\partial N}{\partial y} + g\beta(T - T_{\infty})\cos\gamma + g\beta^*(C - C_{\infty})\cos\gamma - \frac{\sigma B_0^2}{\rho} u$$
(2)

Here along the y-axis, a uniform transverse magnetic field B_0 is placed. Additionally, the induced magnetic field is disregarded, which reduces magnetic Reynolds. Furthermore, electric field and the MHD Hall Effect is ignored.

$$\rho C_p \left(\frac{\partial T}{\partial t} + v \frac{\partial T}{\partial y} \right) = \kappa \frac{\partial^2 T}{\partial y^2} \tag{3}$$

$$\frac{\partial c}{\partial t} + v \frac{\partial c}{\partial y} + \frac{\partial}{\partial y} [V_T (C - C_\infty)] = D_m \frac{\partial^2 c}{\partial y^2}$$
 (4)

$$\frac{\partial N}{\partial t} + v \frac{\partial N}{\partial y} = \frac{\gamma^*}{\rho j} \frac{\partial^2 N}{\partial y^2} - \frac{\tau}{\rho j} \left(2N + \frac{\partial u}{\partial y} \right) \tag{5}$$

Using the continuity equation (1), v can be viewed as either a function of time or a constant. The velocity component stated by Makinde [17] along the y-axis is described as follows-

$$v = -c \left(\frac{v}{t}\right)^{1/2} \tag{6}$$

where c>0 is the suction parameter and c<0 is the injection parameter. Following Qasim et al. [18], the spin gradient viscosity and micro-inertia per unit mass can be defined as follows:

$$\gamma^* = \left(\mu + \frac{\tau}{2}\right)j$$
 and $j = \frac{\mu}{\rho U_0}$ (7)

The thermophoretic parameter was also included in equation (4) by Tsai [19] as-

$$V_T = -\frac{\kappa^{Th}}{T_{ref}} \cdot \frac{\partial T}{\partial y} \tag{8}$$

where K^{Th} represents the thermophoretic coefficient.

Joseph Boussinesq examined buoyancy-driven flow in 1903; he looked into acceleration brought on by gravity and density differences corresponding to buoyancy-driven flow. The density model with a minimal temperature differential between the free stream layer and the wall is shown below-

$$\rho = \rho_{\infty} [1 - \beta (T - T\infty)] \tag{9}$$

where g (ρ - ρ_{∞}) is known as buoyancy term. Applying the above approximation, the buoyancy term is given by-

$$g\beta\rho_{\infty} (T - T_{\infty}) \tag{10}$$

The buoyancy force as well as pressure term is now

expressed as $-\frac{\partial p}{\partial x} = g\beta\rho_{\infty}$ (*T*- T_{∞}). Furthermore, Boussinesq approximation for combined heat and mass transfer convection can be expressed as follows:

$$-\frac{\partial p}{\partial x} = g\beta \rho_{\infty}(T - T_{\infty}) + g\beta^* \rho_{\infty}(C - C_{\infty})$$
 (11) This idea is referred to as the Boussinesq approximation. This approximation suggests that the density variation is too small to be ignored, in accordance with Boussinesq [20].

Then buoyancy model (11) can be modified as-

$$-\frac{\partial p}{\partial x} = g\beta \rho_{\infty}(T_{\infty} - T) + g\beta^* \rho_{\infty}(C_{\infty} - C) \quad (12)$$

According to Animasaun and Anselm [21], $\mu(T) = \mu^* [1 + b \ (T_w - T)]$ which is valid only for $T_w > T_\infty$. Then a modification was given to take the following form - $\mu(T) = \mu^* [1 + b \ (T_\infty - T)]$, where $T_w < T_\infty$ (13)

The impact of temperature on both vortex and dynamic viscosity of micropolar fluid is still being studied by fluid dynamics experts using scientific findings. Using the relations (12) and (13) in equation (2), we obtain-

$$\frac{\partial u}{\partial t} + v \frac{\partial u}{\partial y} = \frac{1}{\rho} \frac{\partial}{\partial y} \left(\mu \frac{\partial u}{\partial y} \right) + \frac{\tau}{\rho} \frac{\partial^2 u}{\partial y^2} + \frac{\tau}{\rho} \frac{\partial N}{\partial y} + g\beta (T_{\infty} - T_{\infty})$$

T)
$$cos\gamma + g\beta^*(C_{\infty} - C)cos\gamma - \frac{\sigma B_0^2}{\rho}u$$
 (14)

(3) implies that,
$$\rho C_p \left(\frac{\partial T}{\partial t} + v \frac{\partial T}{\partial v} \right) = \kappa \frac{\partial^2 T}{\partial v^2}$$
 (15)

Using the equation (12), the equation (4) becomes-

$$\frac{\partial c}{\partial t} + v \frac{\partial c}{\partial v} + \frac{\partial}{\partial v} \left[V_T (C_{\infty} - C) \right] = D_m \frac{\partial^2 c}{\partial v^2}$$
 (16)

Using the equation (7), the equation (5) becomes-

$$\frac{\partial N}{\partial t} + v \frac{\partial N}{\partial y} = \left[\frac{\mu(T)}{\rho} + \frac{\tau}{2\rho} \right] \frac{\partial^2 N}{\partial y^2} - \frac{\tau U_0}{\mu(T)} \left(2N + \frac{\partial u}{\partial y} \right)$$
(17)

Equations (14) - (17) are subjected to the following boundary conditions:

$$u(y,0) = 0$$
 $T(y,0) = T_w$ $N(y,0) = 0$ $C(y,0) = C_w$
for $t \le 0$ (18)

$$u(0,t) = 0$$
 $T(0,t) = T_w$ $N(0,t) = m_0 \frac{\partial u}{\partial t}$ $C(0,t) = C_w$

for
$$t > 0$$
 (19)

$$u(\infty,t) \to U_0 \ T(\infty,t) \to T_\infty \ N(\infty,t) \to 0 \ C(\infty,t) \to C_\infty$$
for $t > 0$ (20)

The above boundary conditions are valid when $T_w < T_\infty$ and $C_w < C_\infty$. In Equation (19) when $m_0 = 0$, we have N(0, t) = 0 which indicates no-spin condition. Thus, it is impossible for the microelements in a concentrated fluid that is close to the wall to spin.

We introduce the following dimensionless variables into (14) - (17):

$$\eta = \frac{y}{2\sqrt{vt}}; f(\eta) = \frac{u}{U_0}; \theta = \frac{T}{T_\infty}; \varphi = \frac{c}{C_\infty}; N = \frac{U_0}{\sqrt{vt}}h(\eta)$$
(21)

Finally, we have the dimensionless non-linear ordinary differential equations as follows:

$$(1 + \xi - \theta \xi + k_1)f'' - \xi \theta' f' + 2(\eta + c)f' + 2k_1h' + G_r\xi(1 - \theta)\cos\gamma + G_c\xi(1 - \phi)\cos\gamma - Mf = 0$$
(22)

$$\theta'' + 2Pr(\eta + c)\theta' = 0 \tag{23}$$

$$\varphi'' + 2S_c(\eta + c)\varphi' - \lambda S_c(1 - \varphi)\theta'' +$$

$$\lambda S_c \theta' \varphi' = 0 \tag{24}$$

$$\left(1 + \xi - \theta \xi + \frac{k_1}{2}\right) h'' + 2(\eta + c)h' + 2h - \frac{8L_1}{1 + \xi - \theta \xi} h - \frac{2L_1}{1 + \xi - \theta \xi} f' = 0$$
(25)

The aforementioned problem also gives the following dimensionless boundary conditions:

$$f(\eta) = 0, \ \theta(\eta) = \theta_w \ (< I), \ h(\eta) = -\frac{1}{4} f'(0), \ \varphi(\eta) = \varphi_w \ (< I)$$

$$at \ \eta = 0 \qquad (26)$$

$$f(\eta) \to I, \quad \theta(\eta) \to I, \quad h(\eta) \to 0, \quad \varphi(\eta) \to I$$

$$as \ \eta \to \infty \qquad (27)$$

where η is the similarity variable, $Gr = \frac{4tg\beta}{U_0b}$ is the thermal Grashof number, $\xi = bT_\infty$ is the variable viscosity parameter, $k_1 = \frac{\tau}{\mu}$ is the micro-rotation parameter, $Gc = \frac{4tg\beta^*}{U_0b}$ is known as the solutal Grashof number, $Pr = \frac{\nu}{\gamma} = \frac{\mu C_p}{\kappa}$ is the Prandtl number, $L_1 = k_1 U_0 t$ is defined as the time dependent microrotation parameter, $\lambda = -\frac{\kappa^{ThT_\infty}}{\nu T_{ref}}$ is the thermophoretic parameter, $M = \frac{4\sigma B_0^2 L_1}{\rho k_1 U_0}$ is the magnetic field parameter, $Sc = \frac{\nu}{D_m}$ is the Schmidt number and γ is the inclined angle of permeable surface with γ -axis, $f(\eta)$ is the dimensionless temperature function, $\varphi(\eta)$ is the dimensionless concentration function, $h(\eta)$ is the dimensionless micro-rotation function.

3. NUMERICAL RESULTS AND DISCUSSION

The effects of Lorentz force and inclined angle on time-dependent free-convective thermal-material transport by micropolar binary mixture of fluid passing a continuous permeable surface have been investigated in this research paper. Initially, using a modified Boussinesq's approximation, the higher order nonlinear partial differential equations (1) – (5) have been converted into second order simultaneous linear ordinary differential equations. Using the similarity technique, it was also transformed into an initial value problem. Finally, numerical solutions have been found for the coupled nonlinear ordinary differential equations (22) - (25) with boundary conditions (26) - (27). Here, the shooting technique has been

implemented using the "MATLAB ODE45" software. The non-dimensional velocity, temperature, concentration, and microrotation profiles are calculated against the dimensionless coordinate η using the aforementioned numerical method, with changes in various thermophysical parameters influencing the fluid flow phenomenon.

Figures (2–3) show the numerical results. The thermo-physical quantities of practical significance, such as the Nusselt number, coefficient of skin friction, and Sherwood number, are also calculated and displayed in tables (1-2) to analyze the internal characteristics of the fluid flow. We have included here the parameters as magnetic parameter (M), and an inclined angle (γ) . It should be noted that only the variation of the selected parameter is performed while the effect of that parameter on the field variables is observed. We have considered the remaining parameters to be constants. We have taken the fixed values of parameters as: $\gamma = 45^{\circ}$, Pr = 0.71, M = 2.0, c= 0.5, L_1 = 0.33, λ = 1.00, Sc = 0.22, ξ = 3.00, K_1 = 0.5, Gr = 10.0, Gc = 10.0. Furthermore, the boundary conditions at infinity have been supposed to apply at a finite point of $\eta = 5.0$.

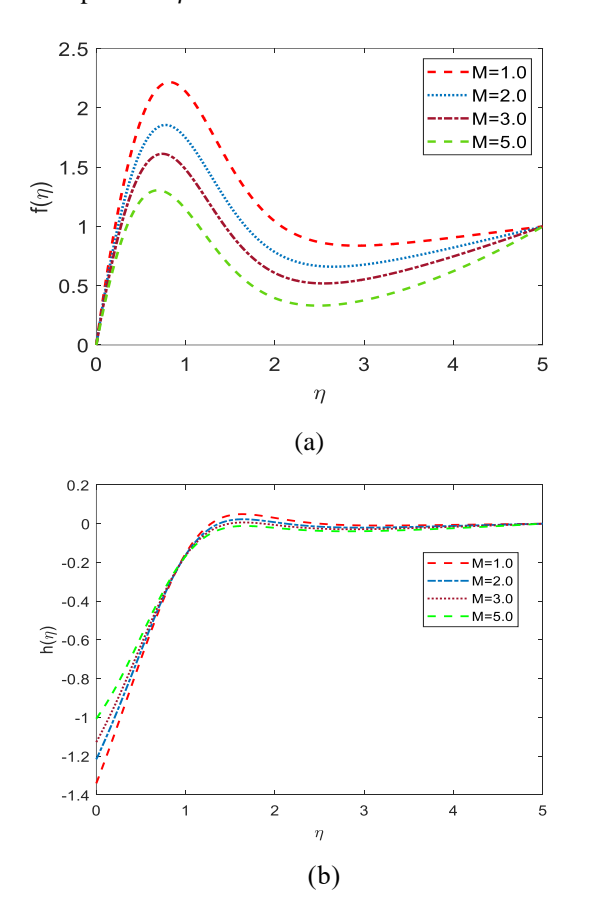


Figure 2: (a) Velocity, and (b) micro-rotation profiles for various values of magnetic parameter (M).

Effect of Lorentz Force

Figure 2 displays the influences of magnetic parameter (M) on fluid velocity and micro-rotation of

fluid particles for several values of magnetic parameter (M). As M gets higher values, the velocity fields get smaller, as can be seen in figure 2(a). This is caused by the Lorentz forces that are created by a transverse magnetic field; these forces act to slow down the fluid motion. Consequently, the fluid velocity gets smaller as the values of M grow due to an increase in Lorentz force or resistive force. It is also clear that the higher value of M corresponds to a small increase of the micro-rotation profiles in a closed proximity to the wall $0.0 \le \eta \le 1.0$ and thereafter they change the behavior and decrease somewhat with increasing M and finally approach zero asymptotically all together.

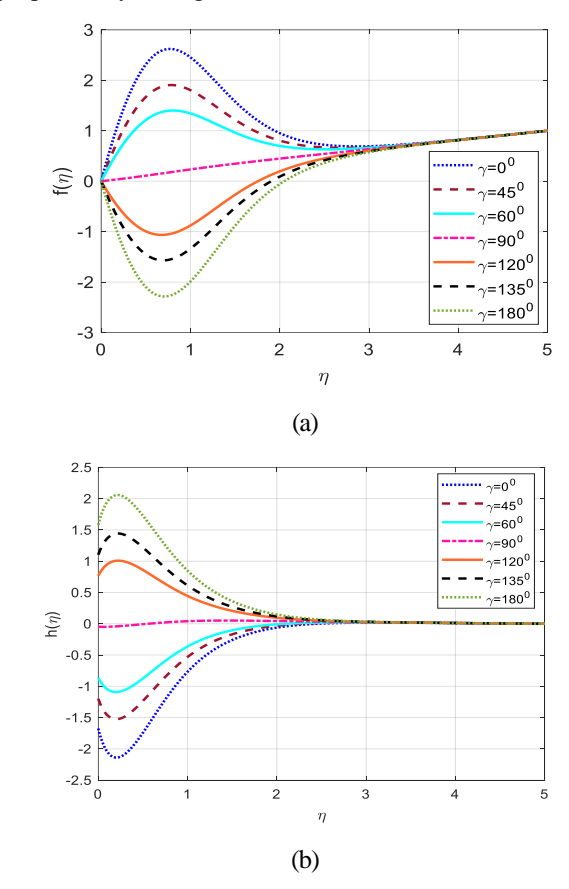


Figure 3: (a) Velocity, and (b) micro-rotation profiles for various values of inclination angle (γ) .

3.1 Effect of Inclination

Figure 3 depicts the effects of inclination angle (γ) on the velocity and micro-rotation profiles. According to figure 3(a), the velocity decreases for the uplifting values of inclined angle (γ). The impact of the buoyancy force decreases as the values of γ upgrade, because of the multiplication factor $\cos \gamma$ and consequently, the velocity decreases rapidly for the increasing value of γ . For horizontal surface ($\gamma = 90^{\circ}$), it is also seen that velocity profile is a strictly monotonic increasing function of η and a symmetrical shape is obtained for other inclined angles. Nevertheless, the figure 3(b) shows an opposite trend for increasing values of γ . Because of the

growing value of γ , the angular momentum of boundary layer increases, which enhances the microrotation profile.

3.2 Skin friction, Nusselt number, Sherwood number and surface couple stress

To further illustrate the internal characteristics of the fluid flow, the thermophysical quantities like Sherwood number (Sh), Nusselt number (Nu), the skin friction coefficient (f'(0)) and the surface couple stress (h'(0)) of practical significance are tabulated as follows:

Table 1: Values of skin friction coefficient, heat and mass transfer rates, surface couple stress for various values of magnetic parameter (M).

М	f'(0)	$-\theta'(0)$	$-\varphi'(0)$	h'(0)
1.0	7.092	1.300	0.825	-6.424
2.0	6.475	1.300	0.825	-5.735
3.0	6.028	1.300	0.825	-5.240
4.0	5.680	1.300	0.825	-4.861

The effects of the magnetic parameter (M) on the coefficient of skin friction, Nusselt number, Sherwood number, and surface couple stress are shown in Table 1. From the tubulated data, it is clear that the coefficient of skin-friction decreases and surface couple stress enhances with the increase of M(1.0-4.0) whereas heat and mass transfer rates remain the same with variation of M(1.0-4.0). We also notice that as M(1.0-4.0) increases, the skin-friction coefficient decreases by about 20% while the surface couple stress increases by about 24%.

Table 2: Values of skin friction coefficient, heat and mass transfer rates, surface couple stress for various values of inclined angle (γ) .

γ	f'(0)	$-\theta'(0)$	$-\varphi'(0)$	h'(0)
0°	6.698	1.300	0.825	-5.934
15°	6.475	1.300	0.825	-5.735
30°	5.825	1.300	0.825	-5.149
45°	4.790	1.300	0.825	-4.217
60°	3.443	1.300	0.825	-3.003

Table 2 describes the impact of inclined angle (γ) on the coefficient of skin-friction, Nusselt number, Sherwood number and surface couple stress. From the table, it is seen that the coefficient of skin-friction decreases and surface couple stress enhances with the increase of $\gamma(0^{\circ} - 60^{\circ})$ whereas heat and mass transfer rates are unchanged with the change of $\gamma(0^{\circ} - 60^{\circ})$. We also notice that the skin-friction coefficient reduces about 49% but the surface couple stress upgrades about 44% in rising of $\gamma(0^{\circ} - 60^{\circ})$.

4. CONCLUSION

This article analyzes the effects of the Lorentz force and inclination angle on the time-dependent free-convective thermal-material transport by a micropolar binary fluid mixture through a continuous permeable surface. We can deduce the following conclusions from our numerical results:

- The Lorentz forces act to slow down the fluid motion.
- Due to the impact of the buoyancy force, the velocity drops rapidly for the rising value of inclined angle (γ); the micro-rotation profile, on the other hand, shows an opposite trend.
- The skin friction coefficient falls by 49%, and 20% due to upturning values of inclined angle γ (0°-60°), and Lorentz force M (1.0 4.0), respectively.
- The surface couple stress is found to be increased about 24%, and 44% with the upturning values of M (1.0 4.0), and γ (0⁰-60⁰), respectively.

Acknowledgement

This study was carried out at the department of Mathematics, Bangladesh University of Engineering and Technology, Dhaka, Bangladesh with funding from the Bangabandhu Science and Technology Fellowship Trust, Ministry of Science and Technology, BCSIR Campus, Dhanmondi, Dhaka.

REFERENCES

- [1] Cheng, C.Y., 2006. Fully developed natural convection heat and mass transfer of a micropolar fluid in a vertical channel with asymmetric wall temperatures and concentrations. International Communications in Heat and Mass Transfer, Volume 33(5), pp.627-635.
- [2] Haque, M.Z., Alam, M.M., Ferdows, M. and Postelnicu, A., 2012. Micropolar fluid behaviors on steady MHD free convection and mass transfer flow with constant heat and mass fluxes, joule heating and viscous dissipation. Journal of King Saud University-Engineering Sciences, Volume 24(2), pp.71-84.
- [3] Ali, M., Nasrin, R. and Alim, M.A., 2021. Analysis of boundary layer nanofluid flow over a stretching permeable wedgeshaped surface with magnetic effect. Journal of Naval Architecture and Marine Engineering, Volume 18(1), pp.11-24.

- [4] Tripathy, R.S., Dash, G.C., Mishra, S.R. and Hoque, M.M., 2016. Numerical analysis of hydromagnetic micropolar fluid along a stretching sheet embedded in porous medium with non-uniform heat source and chemical reaction. Engineering Science and Technology, an International Journal, Volume 19(3), pp.1573-1581.
- [5] Animasaun, I. L., 2016. Double diffusive unsteady convective micropolar flow past a vertical porous plate moving through binary mixture using modified Boussinesq approximation. Ain Shams Engineering Journal, Volume 7(2), pp. 755–765.
- [6] Immaculate, D.L., Muthuraj, R., Selvi, R.K., Srinivas, S. and Shukla, A.K., 2015. The influence of thermophoretic particle deposition on fully developed MHD mixed convective flow in a vertical channel with thermal-diffusion and diffusion-thermo effects. Ain Shams Engineering Journal, Volume 6(2), pp.671-681.
- [7] Ahmed, N., Sengupta, S. and Datta, D., 2013. An exact analysis for MHD free convection mass transfer flow past an oscillating plate embedded in a porous medium with Soret effect. Chemical Engineering Communications, Volume 200(4), pp.494-513.
- [8] Vedavathi, N., Ramakrishna, K. and Reddy, K.J., 2015. Radiation and mass transfer effects on unsteady MHD convective flow past an infinite vertical plate with Dufour and Soret effects. Ain Shams Engineering Journal, Volume 6(1), pp.363-371.
- [9] Prasad, D.K., Chaitanya, G.K. and Raju, R.S., 2019. Double diffusive effects on mixed convection Casson fluid flow past a wavy inclined plate in presence of Darcian porous medium. Results in Engineering, Volume 3, p.100019.
- [10] Ali, M., Alim, M.A., Nasrin, R., Alam, M.S. and Munshi, M.H., 2017. Similarity solution of unsteady MHD boundary layer flow and heat transfer past a moving wedge in a nanofluid using the Buongiorno model. Procedia engineering, Volume 194, pp.407-413.
- [11] Rasool, G. and Wakif, A., 2021. Numerical spectral examination of EMHD mixed convective flow of second-grade nanofluid towards a vertical Riga plate using an advanced version of the revised Buongiorno's nanofluid model. Journal of Thermal Analysis and Calorimetry, Volume 143(3), pp.2379-2393.

- [12] Asogwa, K.K., Alsulami, M.D., Prasannakumara, B.C. and Muhammad, T., 2022. Double diffusive convection and cross diffusion effects on Casson fluid over a Lorentz force driven Riga plate in a porous medium with heat sink: An analytical approach. International Communications in Heat and Mass Transfer, 131, p.105761.
- [13] Ali, M., Alim, M.A., Nasrin, R. and Alam, M.S., 2017. Numerical analysis of heat and mass transfer along a stretching wedge surface. Journal of Naval Architecture and Marine Engineering, Volume 14(2), pp.135-144.
- [14] Li, X., Li, C., Xue, Z. and Tian, X., 2018. Analytical study of transient thermo-mechanical responses of dual-layer skin tissue with variable thermal material properties. International Journal of Thermal Sciences, Volume 124, pp.459-466.
- [15] Kowsalya, J. and Begam, M.J., 2016. MHD Mass transfer flow past a vertical porous plate embedded in a porous medium in a slip flow regime with the influence ff Hall current and thermal diffusion. International Journal of Advanced Scientific and Technical Research, Volume 5(6), pp.600-613.
- [16] Cheng, P., 1964. Two-dimensional radiation gas flow by moment method. American Institute of Aeronautics and Astronautics Journal. Volume 2(9), pp.1662 1664.
- [17] Makinde, O. D., 2005. Free convection flow with thermal radiation and mass transfer past a moving vertical porous plate. International Communications on Heat and Mass transfer, Volume 32(10), pp.1411 – 1419.
- [18] Qasim, M., Khan, I. and Sheltie, S., 2013. Heat transfer in a micropolar fluid over a stretching sheet with Newtonian heating. PloS ONE, Volume 8(4), e59393.
- [19] Tsai, R., Chang, Y.P. and Lin, T.Y., 1998. Combined effects of thermophoresis and electrophoresis on particle deposition onto a wafer. Journal of Aerosol Science, Volume 29(7), pp. 811 825.
- [20] Boussinesq J., 1897. Th'eorie de I, ecoulement tourbillonnant et tumultuex des liquids dans les lots rectilignes a grande section. Gauthier-Villars Paris. Volume 1, Open Library OL 7070543M.
- [21] Animasaun, I. L. and Anselm, O. O., 2014. Effects of variable viscosity, Dufour, Soret and thermal conductivity on free convective heat and mass transfer of non-Darcian flow past porous flat surface. American Journal of Computational Mathematics, Volume 4(4), pp. 357 365.